



Bimetallic coatings synergistically enhance the speeds of photocatalytic TiO₂ micromotors†

Cite this: DOI: 10.1039/d0cc00212g

 Received 9th January 2020,
Accepted 2nd March 2020

DOI: 10.1039/d0cc00212g

rsc.li/chemcomm

 Zuyao Xiao,^a Jingyuan Chen,^a Shifang Duan,^a Xianglong Lv,^a Jizhuang Wang,^b
Xing Ma,^{id} ^{a,c} Jinyao Tang^{id} ^{b,d} and Wei Wang^{id} ^{*a}

The design of powerful, more biocompatible microrobots calls for faster catalytic reactions. Here we demonstrate a two-fold increase in the speed of photocatalytic TiO₂–metal Janus micromotors via a Au/Ag bi-layered coating. Electrochemical measurements show that such a bimetallic coating is a better photocatalyst than either metal alone. Similarly, an additional sputtered Ag layer could also significantly increase the speed of Pt–PS or TiO₂–Pt micromotors, suggesting that applying bimetallic coatings is a generalizable strategy in the design of faster catalytic micromotors.

Recently, many efforts have been devoted to the research of micromotors, due to their potential applications in drug delivery, sensing, environment remediation and other fields.^{1–3} Catalytic reactions, as one of the most useful and convenient approaches to convert chemical energy into motion, has played a significant role and attracted much attention.^{4–10} However, earlier studies show that most catalytic microswimmers suffer from energy-conversion efficiency as low as 10^{−9}.¹¹ An extremely low energy efficiency at this level causes many practical problems, from slow motors of low loading capabilities, to a requirement of high fuel concentrations that often become undesirable. Therefore, improving the efficiency of catalytic microswimmers is imperative for the design of high-performance, biocompatible micromotor in practical use.

One way to improve the efficiency is to increase the roughness of the catalytic surface. For example, PS–Pt or SiO₂–Pt Janus microspheres with a rough Pt coating move faster in H₂O₂ than those with smooth coatings.^{12–14} Similar enhancement has been discovered for photocatalytic micromotors as well. For example,

Pumera *et al.* showed that light-driven ZnO–Pt micromotor with a bumpy surface displayed a remarkable speed-boost over motors with a smooth surface.¹⁵ This approach of surface roughening, although effective, often involves complicated chemical and physical processes.

Alternatively, a few studies have discovered that metal silver (Ag) significantly enhances the speed of catalytic micromotors. For example, the Wang lab showed that bimetallic microrod motors and Pt Janus motors both moved significantly faster in solutions containing trace amount of Ag ions.^{16,17} Moreover, Zhang *et al.* found that jellyfish-shaped micromotors with a Au/Ag/Au tri-layered shell moved faster in H₂O₂ than motors with a single layer of Au or Ag.¹⁸

Inspired by these earlier reports of Ag-induced speed enhancement of catalytic micromotors, we here report a two-fold increase in the speeds of photocatalytic titanium oxide (TiO₂) micromotors, enabled by sequentially depositing a layer of Au followed by sputtering Ag. Electrochemical measurements suggest a synergy between these two metal layers that significantly enhance the photocurrent, possibly by increasing the photocatalytic reaction rate. Several other potential sources of enhancement are also proposed but eliminated. This two-fold speed enhancement, albeit mild, is generalizable and can be easily extended to other catalytic micromotors (such as PS–Pt and TiO₂–Pt motors), and thus hold promise in the design of high-performance micromotors moving in low concentrations of fuels.

The fabrication of the bimetallic, bilayered Janus micromotors, referred to as “TiO₂–Au/Ag”, is shown in Fig. 1a, and details are given in the ESI.† TiO₂ microspheres were first synthesized by a classic solvothermal method, followed by annealing.¹⁹ A monolayer of TiO₂ microspheres was then first coated with 50 nm of Au by electron beam evaporation (yielding TiO₂–Au particles), followed by a layer of Ag by an ion sputter machine (yielding TiO₂–Au/Ag particles). A representative SEM image of the fabricated Janus particles is given in Fig. 1b, EDX elemental mapping is given in Fig. S1 (ESI†). We emphasize the importance of using the sputtering method for the Ag coating, as Ag coatings produced by e-beam evaporator did not lead to speed enhancement

^a School of Materials Science and Engineering, Harbin Institute of Technology (Shenzhen), Shenzhen, Guangdong 518055, China. E-mail: weiwangz@hit.edu.cn

^b Department of Chemistry, The University of Hong Kong, Hong Kong 999077, China

^c Flexible Printed Electronic Technology Center, Harbin Institute of Technology (Shenzhen), Shenzhen, Guangdong 518055, China

^d State Key Laboratory of Synthetic Chemistry, The University of Hong Kong, Hong Kong 999077, China

† Electronic supplementary information (ESI) available. See DOI: 10.1039/d0cc00212g

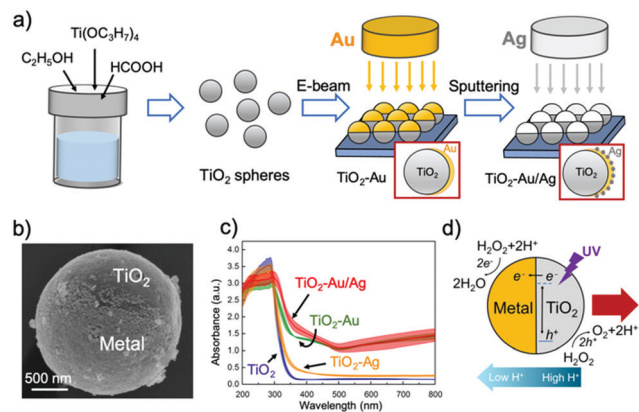


Fig. 1 Preparation and propulsion mechanism of photocatalytic TiO_2 -Au/Ag Janus micromotors. (a) Fabrication of TiO_2 -metal Janus micromotors (see main text and ESI† for details) Insets with red boxes: cross-sectional cartoon of the produced Janus particles. (b) SEM image of a TiO_2 -metal Janus microsphere. (c) UV-vis light absorption spectra of TiO_2 thin films coated with various materials. Shaded error bars represent the standard deviation of measurements from three samples for each material. Background absorption has been subtracted. (d) Schematic of a TiO_2 -metal Janus micromotor undergoing self-electrophoresis (see main text for details).

(Fig. S2, ESI†). This is likely because sputtering technique in our case produced a rough surface with small Ag nanoparticles, as seen in Fig. 3c.

TiO_2 -metal Janus micromotors move by a self-electrophoresis mechanism (Fig. 1d).^{20,21} To briefly explain, TiO_2 , as a photo-sensitive semiconductor, absorbs light of certain wavelengths corresponding to its bandgap. The light absorption spectra of pure TiO_2 , TiO_2 coated with Au or Ag, and TiO_2 coated with a Au/Ag bilayer are given in Fig. 1c (see ESI† for details on sample preparation and measurement), showing strongest absorption in the UV regime. Photons absorbed then generate electron/hole pairs inside the TiO_2 , which reduce and oxidize water into hydrogen and oxygen gas, respectively. In doing so, a concentration gradient of protons across the motor builds a self-generated local electric field that moves the negatively-charged microsphere with the TiO_2 hemisphere leading. Similar redox reactions happen in the presence of H_2O_2 and propel motors faster because of the more favorable electrochemical potential of H_2O_2 .

Our key, and somewhat surprising, observation is that, when illuminated with UV light (365 nm, see ESI† for experiment details), TiO_2 -Au/Ag Janus micromotors moved in H_2O_2 roughly twice as fast as TiO_2 /Au Janus micromotors without the sputtered Ag layer. Representative particle trajectories and speeds are demonstrated in Fig. 2a and b, respectively. In addition, we also examined the dynamics of TiO_2 -Ag motors and pure TiO_2 microspheres under the same experimental condition, and found that TiO_2 -Ag Janus micromotors moved at speeds similar to TiO_2 -Au motors, while pure TiO_2 only exhibited Brownian motion. The dynamics of these four types of particles in H_2O_2 are shown in Video S1 (ESI†).

This enhancement of mobility is also noticeable even in pure water under UV illumination (Video S2, ESI†). The apparent diffusion coefficients (D) of the same three types of motors as

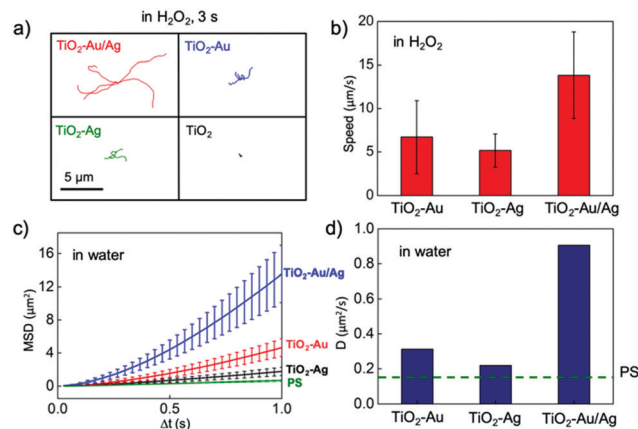


Fig. 2 Tracking the motion of TiO_2 -metal micromotors. (a) Representative trajectories of pure TiO_2 , TiO_2 /Au, TiO_2 /Ag and TiO_2 -Au/Ag microspheres moving in 0.5% H_2O_2 for 3 s. (b) Average speeds of TiO_2 -Au, TiO_2 -Ag and TiO_2 -Au/Ag micromotors moving in 0.5% H_2O_2 . Error bars are the standard deviation from 20 particles. (c) Mean square displacement of three types of TiO_2 -metal Janus motors moving in water. Error bars are the standard deviation from 50 particles. (d) Apparent diffusion coefficients of the three types of motors extracted from (c). The diffusion coefficient of polystyrene microspheres of comparable sizes is marked with a green dashed line. In all these experiments, UV light of 600 mW cm^{-2} was applied.

studied in H_2O_2 , namely TiO_2 -Au/Ag, TiO_2 -Au and TiO_2 -Ag, were extracted from mean squared displacement (MSD) measurement by fitting Fig. 2c with eqn (1),

$$\text{MSD} = 4D\tau + V^2\tau^2 \quad (1)$$

where τ is the time interval and V is the propulsion speed. Results show that, even in pure water, TiO_2 -Au/Ag micromotors are still more active than TiO_2 -Au motors or TiO_2 -Ag motors (Fig. 2d). Control experiments eliminated possibilities of drift or convection (Fig. S8, S9 and Video S4, ESI†). Fig. 3a and b show that, with the increase of light intensity and fuel concentration, the motors exhibited a higher speed, typical for photocatalytic micromotors.

Interestingly, we discovered that the sputtering time of Ag had a substantial influence on the speeds of the TiO_2 -Au/Ag motors (Fig. 3c). More precisely, Ag layers of various morphologies were produced at different sputtering time, from island-like Ag nanoparticles at short sputtering time (*e.g.* 10 s), to large domains of Ag particles that have seemingly annealed together at long sputtering time (*e.g.* 200 s). Cross sectional SEM images are given in Fig. S3 (ESI†). The motor speed reached a maximum at intermediate sputtering time of 50–100 s, corresponding to a Ag film in transition between the above two morphologies. Qualitatively, we speculate that the presence of Ag nanoparticles is important for enhancing the catalytic performance. An intermediate sputtering time might have struck the right balance between Ag morphologies and amount.

The significant enhancement of TiO_2 -Au/Ag Janus motors over similar TiO_2 motors coated with one metal naturally piques our curiosity. In the remainder of this article, we detail our efforts in unravelling this mystery, by raising and eliminating a series of possibilities, culminating in an argument of photocatalytic synergy in the end.

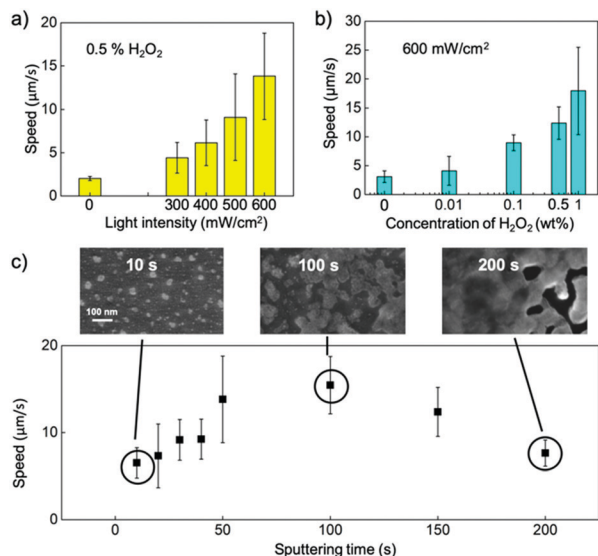


Fig. 3 The speeds of TiO_2 -Au/Ag motors under different light intensities (a) and in different H_2O_2 concentrations (b). (c) The influence of the Ag layer sputtering time on the speed of TiO_2 -Au/Ag micromotors. Inset: Representative morphologies of the sputtered Ag films acquired at different sputtering time (see Fig. S2 for cross-sectional views and thickness information, ESI †). Error bars in (a) and (b) are the standard deviation from 20 particles.

The first possibility argues that, by coating Ag, which is known to be a good catalyst towards decomposing H_2O_2 even without light, a TiO_2 -Au/Ag becomes dually propelled in H_2O_2 : light moves it toward TiO_2 , and so does the chemical propulsion similar to PS-Pt Janus micromotors.^{4,22} Hence, by combining two different power sources pointing in the same direction, the total speed of TiO_2 -Au/Ag Janus motors is higher than TiO_2 coated with either metal. However, the simple fact that TiO_2 -Au/Ag Janus particles only exhibited Brownian motion in H_2O_2 without illumination, shown in Video S3 (ESI †), suggests that the sputtered Ag layer is not capable of chemically powering the motor in H_2O_2 , thus eliminating this possibility.

The second possibility is that, since the photocatalytic performance of a TiO_2 -metal micromotor is sensitive to the choice of the cathode materials,^{20,23,24} Ag might be a more effective photocathode than Au. The metal coating is likely changed from Au to Ag upon sputtering, thereby enhancing photocatalysis. This argument, if true, naturally suggests that a TiO_2 -Ag motor would move faster than a TiO_2 -Au motor under the same experimental condition, yet experiments in both H_2O_2 and water (Fig. 2) show that they have comparable activities. The above two arguments, that Ag alone gives rise to a speed enhancement for one reason or the other, are thus proven incorrect.

Instead, our results suggest the Au and Ag coatings work in synergy to enhance the speed of TiO_2 motors under UV light. A few important clues of this synergy are worth noting. First, this synergy does not need the participation of H_2O_2 , shown by the fact that TiO_2 -Au/Ag motors are more active than TiO_2 -Au or TiO_2 -Ag motors even in pure water. This is unlike previous studies of synergetic propulsion of Ag-Au¹⁶ or Ag-Pt¹⁷ motors

in H_2O_2 , and strongly suggests that the synergy in our system comes not from a catalytic enhancement specific to H_2O_2 , but something more generalizable. Furthermore, this synergy does not change the photocatalysis mechanism of a TiO_2 micromotor, since the speed of a TiO_2 -Au/Ag micromotor still scales with increasing light intensities (shown in Fig. 3a).

There are two possible origins for this synergy, one related to light absorption, and the other related to catalysis. We first considered the possibility that TiO_2 microspheres with bilayered coating absorbs light better than those with a single metal coating. This possibility arises because the island Ag nanoparticles produced by sputtering, as well as the Au thin film deposited by evaporation, are both known to be strong light absorbers due to the surface plasmon resonance (SPR) effect. Could this effect influence motor performance in our case? A closer look at the light absorption spectra in Fig. 1c, however, revealed that there is no significant difference in the light absorption between TiO_2 -Au and TiO_2 -Au/Ag. This argument of a synergistic light absorption is therefore unlikely.

Finally, we postulate that the combination of a Au layer with island-Ag particles shows a superior photocatalytic performance over either layer alone. A direct evidence comes from the measurements of the photocurrents between a TiO_2 anode and a metal cathode (Fig. 4, see ESI † for experiment details and Fig. S4, S5 for more results).

It is clear from the data presented in Fig. 4 that the photocurrent between a Au/Ag photocathode and a TiO_2 photoanode was much larger than that measured with a Au or Ag electrode. Because the motor speed scales linearly with the photocurrent in the classic self-electrophoresis mechanism for TiO_2 motors,²¹ it is fair to speculate that the higher photocurrent generated in an electrochemical cell with a Au/Ag photocathode, which corresponds to a TiO_2 motor coated with Au then sputtered with Ag, would lead to a faster motor.

Similar synergistic enhancement by a bimetallic catalyst is well-documented in the literature. In particular, Au/Ag bimetallic catalysts show better performance than single metal for a variety of reactions.²⁵⁻²⁸ These studies offer a few possible mechanisms for the observed synergy between Au and Ag coatings in our

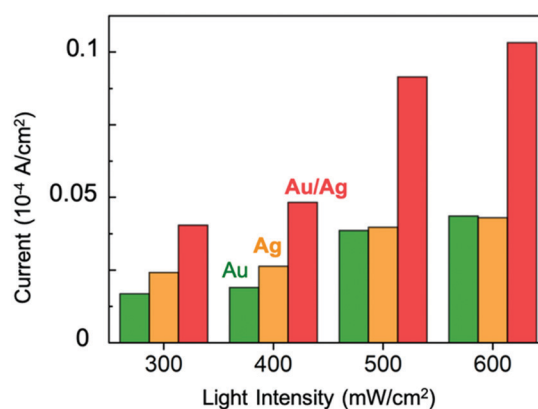


Fig. 4 Photocurrent of electrochemical cells with a TiO_2 anode and various metals as the cathode, at different light intensities.

experiments. First, Ag–Au alloy is known to be of a higher step density than Ag or Au, arising from lattice deformation due to the misfit of atom sizes between Ag and Au. With the contribution of both lattice deformation and surface roughening, more dangling bonds are present on the surface, leading to a higher adsorption of reactant and consequently better catalysis.²⁹ Second, because Ag has a smaller work function than Au, the presence of Ag on the surface of Au may promote the transfer rate of electrons from TiO₂ to the metal layer, accelerating the reduction of hydrogen peroxide.³⁰ The third possibility is that the presence of Ag modified the electronic structure of Au, shifting its d-band center.³¹ This lessens the adsorption of oxygen on the metal surface and facilitates the reduction of hydrogen peroxide intermediates, thereby enhancing the photocurrent. The shifting of d-band centre was recently proposed by Chen *et al.* to explain a significant speed increase of SiO₂–Pt micromotors decorated with Ag nanoparticles.¹⁷ These three mechanisms could all contribute to varying degrees, yet elucidating the exact mechanism is beyond the scope of this communication.

Before we conclude, we confirm that this synergy between one catalytic layer with a second, sputtered layer of Ag, can be applied to other types of micromotors. For example, by sputtering Ag on a PS–Pt micromotor that moves in H₂O₂, and a TiO₂–Pt micromotor that moves in water under UV light, we see an increase of speed by 65% and 31%, respectively (Fig. S6 and S7, ESI†). These results show that the enhancement by Ag is not limited to the metal of Au, or limited to scenarios involving light propulsion, and can thus be generalized to a wide range of catalytic micromotors.

In conclusion, we report a light-driven, bilayered TiO₂–Au/Ag Janus micromotor, fabricated by sputtering Ag on top of an evaporated Au layer, that moves twice as fast as TiO₂–Au or TiO₂–Ag Janus micromotors in both H₂O₂ and pure water. Electrochemical measurements reveal a significant increase in the photocurrent between a TiO₂ photoanode and a Au/Ag photocathode over samples with only one metal coating. This enhancement by bimetallic coating could arise from lattice mismatch, a lower work function of Ag than Au, or a shift of d-band centre in Au, which leads to an enhancement in the catalytic activity of the metal coating and ultimately a faster motor. This bilayered, bimetallic design can be exploited to boost the performance of a broad range of catalytic micromotors, and may contribute to the designs of highly efficient microswimmers that move faster, load more, and consume less fuels. Future studies could apply this design in biocompatible fuels such as urea or glucose.^{32,33}

This project is financially supported by the National Natural Science Foundation of China (11774075, 51802060), the Natural Science Foundation of Guangdong Province (No. 2017B030306005), the Shenzhen Innovation Project (KQJSCX20170726104623185), the Shenzhen Peacock Group (KQTD20170809110344233), and the Shenzhen-Hong Kong Innovation Circle Program (SGDX2019081623341332).

Conflicts of interest

There are no conflicts to declare.

Notes and references

- 1 J. Wang, *Nanomachines: Fundamentals and Applications*, John Wiley & Sons, 2013.
- 2 B. Jurado-Sánchez and J. Wang, *Environ. Sci.: Nano*, 2018, **5**, 1530–1544.
- 3 K. Yuan, Z. Jiang, B. Jurado-Sánchez and A. Escarpa, *Chem. – Eur. J.*, 2020, **26**(11), 2309–2326.
- 4 J. R. Howse, R. A. Jones, A. J. Ryan, T. Gough, R. Vafabakhsh and R. Golestanian, *Phys. Rev. Lett.*, 2007, **99**, 048102.
- 5 W. F. Paxton, K. C. Kistler, C. C. Olmeda, A. Sen, S. K. Angelo, Y. Cao, T. E. Mallouk, P. E. Lammert and V. H. Crespi, *J. Am. Chem. Soc.*, 2004, **126**, 13424–13431.
- 6 K. K. Dey and A. Sen, *J. Am. Chem. Soc.*, 2017, **139**, 7666–7676.
- 7 K. K. Dey, F. Wong, A. Altemose and A. Sen, *Curr. Opin. Colloid Interface Sci.*, 2016, **21**, 4–13.
- 8 S. Sánchez, L. Soler and J. Katuri, *Angew. Chem., Int. Ed.*, 2015, **54**, 1414–1444.
- 9 J. G. S. Moo and M. Pumera, *Chem. – Eur. J.*, 2015, **21**, 58–72.
- 10 B. Robertson, M.-J. Huang, J.-X. Chen and R. Kapral, *Acc. Chem. Res.*, 2018, **51**, 2355–2364.
- 11 W. Wang, T.-Y. Chiang, D. Velegol and T. E. Mallouk, *J. Am. Chem. Soc.*, 2013, **135**, 10557–10565.
- 12 S. Wang and N. Wu, *Langmuir*, 2014, **30**, 3477–3486.
- 13 U. Choudhury, L. Soler, J. G. Gibbs, S. Sanchez and P. Fischer, *Chem. Commun.*, 2015, **51**, 8660–8663.
- 14 B. Jurado-Sánchez, S. Sattayasamitsathit, W. Gao, L. Santos, Y. Fedorak, V. V. Singh, J. Orozco, M. Galarnyk and J. Wang, *Small*, 2015, **11**, 499–506.
- 15 A. M. Pourrahimi, K. Villa, C. L. Manzanares Palenzuela, Y. Ying, Z. Sofer and M. Pumera, *Adv. Funct. Mater.*, 2019, 1808678.
- 16 D. Kagan, P. Calvo-Marzal, S. Balasubramanian, S. Sattayasamitsathit, K. M. Manesh, G.-U. Flechsig and J. Wang, *J. Am. Chem. Soc.*, 2009, **131**, 12082–12083.
- 17 C. Chen, X. Chang, H. Teymourian, D. E. Ramírez-Herrera, B. Esteban-Fernández de Ávila, X. Lu, J. Li, S. He, C. Fang and Y. Liang, *Angew. Chem., Int. Ed.*, 2018, **57**, 241–245.
- 18 X. Zhang, C. Chen, J. Wu and H. Ju, *ACS Appl. Mater. Interfaces*, 2019, **11**, 13581–13588.
- 19 K. He, G. Zhao and G. Han, *CrystEngComm*, 2014, **16**, 7881–7884.
- 20 R. Dong, Q. Zhang, W. Gao, A. Pei and B. Ren, *ACS Nano*, 2015, **10**, 839–844.
- 21 F. Mou, L. Kong, C. Chen, Z. Chen, L. Xu and J. Guan, *Nanoscale*, 2016, **8**, 4976–4983.
- 22 S. J. Ebbens and J. R. Howse, *Langmuir*, 2011, **27**, 12293–12296.
- 23 Y. Ma, X. Wang, Y. Jia, X. Chen, H. Han and C. Li, *Chem. Rev.*, 2014, **114**, 9987–10043.
- 24 T. Maric, M. Z. M. Nasir, R. D. Webster and M. Pumera, *Adv. Funct. Mater.*, 2020, 1908614.
- 25 J. Zheng, H. Lin, Y.-N. Wang, X. Zheng, X. Duan and Y. Yuan, *J. Catal.*, 2013, **297**, 110–118.
- 26 A. Sandoval, A. Aguilar, C. Louis, A. Traverse and R. Zanella, *J. Catal.*, 2011, **281**, 40–49.
- 27 F. Gauthard, F. Epron and J. Barbier, *J. Catal.*, 2003, **220**, 182–191.
- 28 A. Wang, X. Y. Liu, C.-Y. Mou and T. Zhang, *J. Catal.*, 2013, **308**, 258–271.
- 29 R. Zeis, T. Lei, K. Sieradzki, J. Snyder and J. Erlebacher, *J. Catal.*, 2008, **253**, 132–138.
- 30 A.-Q. Wang, J.-H. Liu, S. Lin, T.-S. Lin and C.-Y. Mou, *J. Catal.*, 2005, **233**, 186–197.
- 31 B. Hammer and J. K. Nørskov, *Advances in Catalysis*, Elsevier, 2000, vol. 45, pp. 71–129.
- 32 Q. Wang, R. Dong, C. Wang, S. Xu, D. Chen, Y. Liang, B. Ren, W. Gao and Y. Cai, *ACS Appl. Mater. Interfaces*, 2019, **11**, 6201–6207.
- 33 M. Pacheco, B. Jurado-Sánchez and A. Escarpa, *Angew. Chem., Int. Ed.*, 2019, **58**, 18017–18024.